JBUON 2021; 26(5): 1931-1941
ISSN: 1107-0625, online ISSN: 2241-6293 • www.jbuon.com
Email: editorial_office@jbuon.com

ORIGINAL ARTICLE

Characterization of the m6A-related lncRNA signature in predicting prognosis and immune response in patients with colon cancer

Shujia Chen[1], Xiaofei Li[2], Lianyi Guo[2], Jiachen Zhang[1], Li Li[1], Xueqiu Wang[1], Yinghui Zhu[2], Jiwei Wang[3]

[1]Department of Gastroenterology, Panjin Central Hospital Affiliated to Jinzhou Medical University, Panjin 124013, China. [2]Department of Gastroenterology, the First Affiliated Hospital of Jinzhou Medical University, Jinzhou 121001, China. [3]Department of Gastrointestinal surgery, Xuzhou Central Hospital, Xuzhou 221009, China

*Shujia Chen, Xiaofei Li and Lianyi Guo contributed equally to this work.

Summary

Purpose: *Colon adenocarcinoma (COAD) is globally one of the most frequently occurring malignant tumors. The patients' 5-year survival rate with colon cancer was poor. There is a usual form of mRNA modification called N6-methyl adenosine (m6A). It is adjusted by the m6A RNA methylation modulator. Nevertheless, few studies of COAD can fully discuss m6A-related lncRNAs' prognostic function.*

Methods: *From the Cancer Genome Atlas (TCGA) database, this study of COAD samples discussed 23 m6A regulator-related lncRNAs systemically. 2 m6A patterns with various clinical results were recognized, and a remarkable correlation between various m6A clusters and tumor immune microenvironment was discovered.*

Results: *According to prognostic analysis, cluster1 had a higher immune checkpoint programmed death-ligand 1 (PD-L1) expression and a better prognosis. A 6 m6A-related lncRNAs model was constructed through least absolute shrinkage and selection operator (LASSO), univariate, multivariate Cox regression and stratified analysis. The outcomes reported that compared with the low-risk group, high-risk groups that were based on model closely were related to poor overall survival (OS). The study ensured a risk model consisting of 6 m6A-related lncRNAs as independent prognosis predictors. For the expression differences between the two groups, Genomes Pathway Analysis, Kyoto Encyclopedia of Genes (KEGG) and Gene Ontology (GO) biological process analyses were conducted. In addition, on the basis of full analysis of OS, a nomogram based on gender, age, lncRNA feature and the stage was constructed. One year, two years, and three years are the periods when the calibration chart performed best.*

Conclusions: *The outcomes of the study confirmed the underlying function of m6A-related lncRNAs and offered fresh perspectives to COAD prognosis.*

Key words: *N6-methyl adenosine (m6A), long non-coding RNAs, prognosis, immune response*

Introduction

As the globally most usual malignant tumors, the second dominant induction of cancer-related deaths is colon adenocarcinoma (COAD) with 1,148,515 new cases in 2020 [1]. Surgery, diagnosis, molecular therapy and radiotherapy continue to improve, and the COAD patients' clinical results have promoted remarkably [2]. Because of the high heterogeneity of colon cancer, the prognosis may vary significantly between patients. The clinical and molecular heterogeneity of colon cancer pre-

Corresponding author: Dr. Jiwei Wang. Department of Gastrointestinal Surgery, Xuzhou Central Hospital, Xuzhou, Jiangsu 221009, China.
Tel: +86 017310923623; Email: 17310923623m@sina.cn
Received: 15/05/2021; Accepted: 18/07/2021

sents a high degree of complexity in progression, development, and response to treatment [3]. Nevertheless, 5-year survival rate is still very low [4]. Therefore, the prognosis of colorectal cancer (CRC) patients must be identified and predicted by new biomarkers, and proper treatment targets and treatment groups must be determined.

In expressing post-transcriptional gene modification, RNA modification exerted a significant function. The most frequent one is the N6-methyladenosine (m6A) modification, which was widely researched [5]. RNA metabolism was influenced by m6A methylation in various aspects, covering translocation, RNA splicing, stability, translocation, stability, and conversion to protein [6]. m6A modification is the process that is invertible and dynamic. It involves signal transduction enzyme, methyltransferase, and demethylase, regarded as "reader", "writer", and "eraser" respectively [7]. KIAA1429, Metttl3, Metttl14, WTAP, ZC3H13 and RBM15 formed a methyltransferase complex, which mediates the process of RNA methylation modification. ALKBH5 and FTO constitute a demethylase that mediates the process of RNA demethylation. YTHDF1, YTHDF2, YTHDC1, YTHDC2 and HNRNPC are involved in signal transduction enzymes. They exert the function in "reading" information of RNA methylation and the translating and degrading downstream RNA [8]. Recently, it was found that many human diseases, particularly cancer, are related to the M6A methylation's abnormal modification closely, covering gastric, hepatocellular and colorectal cancers [6]. However, its specific mechanism needs further study.

Although nearly 60,000 genes can be transcribed in the human genome, protein-coding genes account for approximately 20,000 genes, and most of the rest are non-coding genes. Long non-coding RNAs (lncRNAs) account for one-quarter of the total genes [9]. In recent years, accumulating evidence has shown that lncRNAs play an important role in different biological processes, either *in vivo* or *in vitro*. In particular, abnormal expression of lncRNAs has demonstrated its influence on tumor metastasis, tumor progression and cell proliferation [10]. The abnormal presentation of lncRNAs has been reported lately as a prognostic and diagnostic tumor marker [11], whereas, there were few reports showing the function of lncRNAs in m6A modification in COAD.

From the Cancer Genome Atlas (TCGA) database, the expression profiles of lncRNAs and 23M6a genes among colon cancer patients were extracted by this study. Then, Pearson's correlation analysis was used to distinguish M6a-related lncRNAs. In order to forecast the overall survival (OS) using this pipeline, the model was developed based on a new prognostic model of M6A and found that it is a prognostic model independent of other clinical traits and provides a new approach for the treatment and drug target screening of colon cancer.

Methods

Data collection

Using TCGA database (TCGA, https://portal.gdc.cancer.gov/), this study downloaded transcriptome RNA data sets and related COAD clinical information. According to human genome annotated data, we divided the expression matrix into lncRNA genes and protein-coding genes.

Clustering of m6A regulators

23 m6A methylation regulators were selected, covering 13 readers (YTHDF1, HNRNPC, YTHDF2, HNRNPA2B1, YTHDF3, YTHDC1, YTHDC2, FMR1, LRPPRC, IGFBP1, IGFBP2, IGFBP3, and ELAVL1), eight writers (RBM15B, ZC3H13, METTL3, METTL14, VIRMA, RBM15, WTAP, and METTL16), and two erasers (FTO, ALKBH5) from previously published papers [12-14]. For estimating the correlation between lncRNAs and m6A regulatory genes, this study utilized the Pearson's correlation coefficient. The absolute correlation coefficient is >0.4, and the p value <0.001. lncRNAs were regarded as m6A related lncRNAs. According to the 23 m6A modulators expression ConsensusClusterPlus, this study adopted the R package in order to perform cluster analysis. Through 1000 cycles of calculation, this study got the optimal K-means clustering ("k means" function in R) [15]. Also, to measure the OS, we used the Kaplan-Meier method between different clusters as well. We further explored the association between clusters and clinical characteristics.

Immune cell infiltration

We used the ESTIMATE algorithm (https://bioinformatics.mdanderson.org/public-software/estimate/) to measure the research, evaluated point, and discuss the tumor microenvironment (TME) matrix point to research the degree of two subgroups of immune cell infiltration [16]. The CIBERSORT software package (https://cibersort.stanford.edu/) was adopted to estimate the proportion of 22 samples of immune cell subtypes for analyzing group distinction on immune cell subtypes. P<0.05 was used for further analysis.

Risk Model Construction

Univariate and multivariate regression analyses in the entire TCGA group were first adopted to discuss m6A-related lncRNAs prognosis. Seventeen independent prognostic lncRNAs related to m6A were screened. We randomly divided all sets into the testing group and training group. Analysis of Lasso Cox regression was used to test the correlation between the prognostic features of m6A and the risk of patients in the COAD training group in order to increase the interpredictabil-

ity and accuracy of the statistical prediction model. Finally, six m6A-related lncRNAs were used to build the optimal prognostic model. The following formula was used to calculate every COAD patients' risk point: risk point=ΣExpi *βi. βi stands for each lncRNA coefficient, and Expi stands for each lncRNA presentation. The median risk point cut-off method based on the predictive model was used to separate patients into high-risk set and low-risk set. Then, to assess the prognostic model's availability, this study adopted the Kaplan-Meier survival method. In addition, for improving the prognostic accuracy of the evaluation feature construction, we adopted the salient features and sensitivity of the receiver operating characteristic (ROC) curve.

Independence of the m6A-related lncRNAs model

For detecting whether the prognostic model in the training group was an independent variable regarding other clinical features (age, gender, stage), we used univariate and multivariate Cox regression and stratified analysis. Similarly, selected m6A-related lncRNAs' prognostic value was verified through analyzing the testing set and all TCGA set. Furthermore, we deeply discussed the association between risk points and clinical features.

Enrichment analysis

Kyoto Encyclopedia of Genes and Genomes (KEGG) and Gene Ontology (GO) biological processes were applied for studying the pathways enriched in the two groups [17,18].

Establishing and proving a predictive nomogram

This study established other predictive factors (gender, age, risk point, stage), nomograph and predictive ability of 1-year, 2-year, and 3-year OS [19]. After the calibration curve tested by Hosmer-Lemeshow, we used it to elaborate the consistency between the actual results and the model predicted results.

Statistics

R software (version 4.0.3) analyzed most of the study. We counted the prognostic data of 95% confidence interval (CI) and hazard ratio (HR) in OS. Kaplan-Meier method and log-rank test were also used for contrasting OS between groups, according to the m6A-related lncRNAs presentation. For evaluating the independent prognostic value of OS clinical characteristic, we used univariate and multivariate Cox proportional hazards

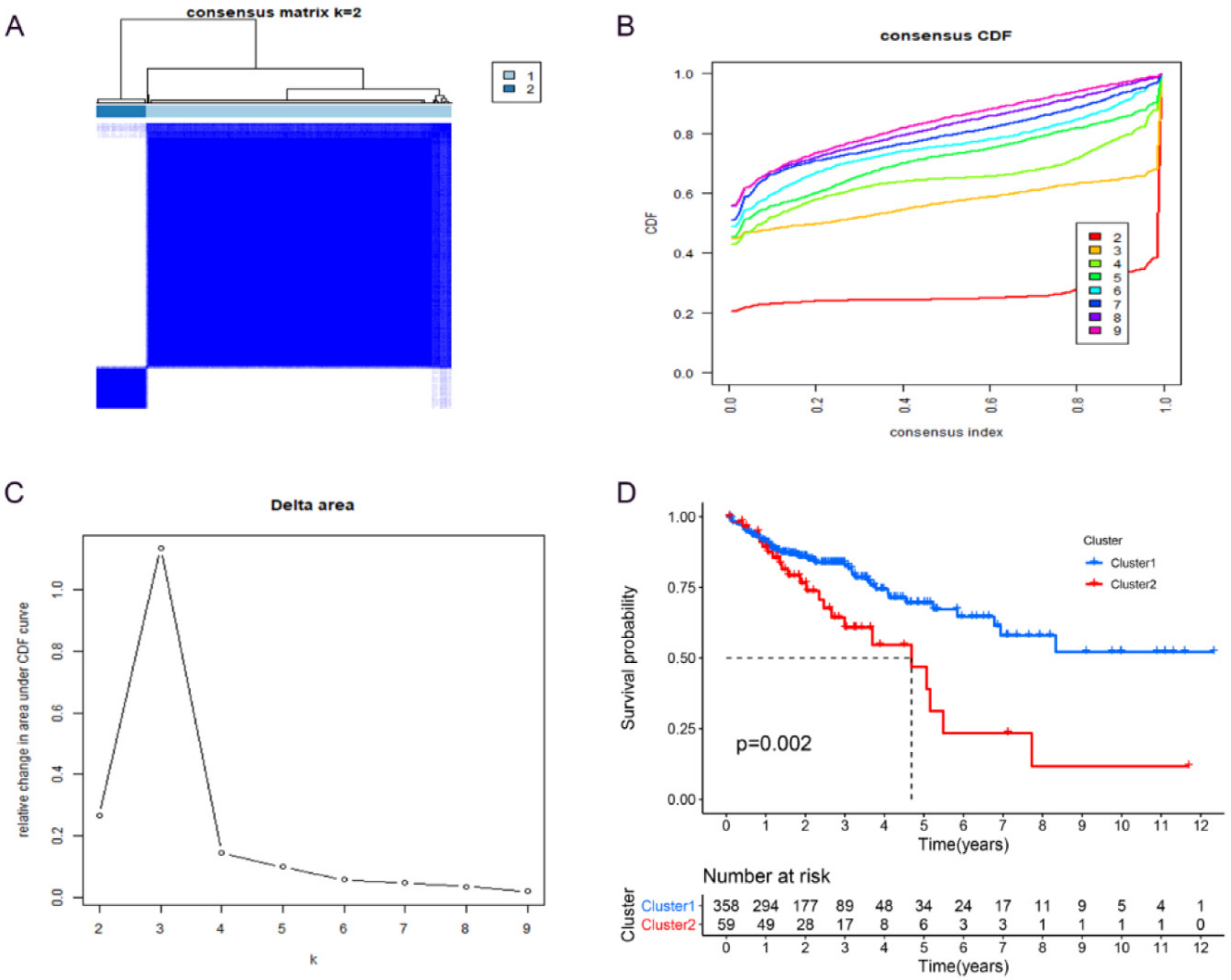

Figure 1. Consensus clustering of m6A genes. **A:** Consensus clustering matrix for k=2. **B, C:** Consensus clustering in relative change area CDF under CDF curve for k=2 to 9. **D:** Kaplan-Meier curves of OS in COAD for two clusters.

regression. In order to assess the 1/2/3-year OS prediction model's prognostic ability, we used the ROC curve (R package "timeROC") and the area under the curve (AUC). We used Fisher's exact test or x^2 to discuss clinical information. All p values were two-sided, and p<0.05 showed statistical significance.

Results

Identification of m6A-related lncRNAs in patients with COAD

From the TCGA database, we screened 23 m6A genes matrix expression and 13150 lncRNAs. m6A-related lncRNAs were defined as those that were remarkably associated with one of 23 m6A genes or more (Pearson R> 0.4 and p <0.001). Eventually, 1,506 m6A-related lncRNAs were discerned as m6A-related lncRNAs. We afterwards performed univariate Cox regression analysis to identify 33 lncRNAs (AL391422.4, AC069222.1, AC139149.1, AC147651.1, AC073111.1, AC104794.2, CAPN10-DT, RPARP-AS1, AC006042.1, U91328.1, AC003101.2, AC069281.2, AL161729.4, ITGB1-DT, AC019205.1, AC008760.1, AP006621.2, AC012360.3, AP001619.1, AL391684.1, AC026367.1, AC245041.1, AC008764.8, AL512306.3, AC156455.1, ZKSCAN2-DT, AC074117.1, NIFK-AS1, AC145285.2, ATP2B1-AS1, AL138921.1, AL359091.4, MALINC1) associated with prognosis. The details are shown in Supplementary Table 1.

Consensus clustering of m6A-related lncRNAs in two clusters

We screened out m6A-related lncRNAs consistent expression, according to the ConsensusClusterPlus R package (http://bioconductor.org/packages/release/bioc/html/ConsensusClusterPlus.html), and divided the COAD cohort into different groups. It was minimal for the crossover between COAD samples when the uniform matrix K value was 2 (Figures 1A, B, and C). The distinction between various clusters in OS was counted by the Kaplan-Meier method. Compared with cluster 2, the OS of cluster 1 patients was significantly better (Figure 1D). We in-depth investigated the correlation between the clusters and clinical signature, and the outcomes showed that the clusters had no correlation with the clinical characteristics such as age, tumor stage, etc. (Supplementary Figure 1A). Then, the correlation between immunotherapy biomarkers and m6A-related lncRNAs clusters was studied. Interestingly, we found that there was no difference in PD-L1 expression between the tumor and non-tumor groups, but in our clusters PD-L1 expression was higher in cluster 1, suggesting that cluster 1 was more responsive to immunotherapy (Supplementary Figure 1B, C). We further explored the correlation between m6A-related lncRNAs and PD-L1, and the results are shown in Supplementary Figure 1D. The asterisk indicated p < 0.05. Positive correlation was shown in red and negative correlation was shown in blue.

Immune infiltration between clusters

The matrix and immune points of all COAD samples were assessed by the ESTIMATE algorithm. The immune points between m6A clusters were greatly diverse. The highest immune point appeared in cluster 1 (Figure 2B). By calculating stromal (Figure 2C) points and ESTIMATE (Figure 2A), compared to cluster2, the cluster1 expression was higher. There were differences between the tumor purity allocation and the immune and stromal, and ESTIMATE points, and tumor purity was usually opposite to the ESTIMATE score, so we inferred that the tumor purity score of cluster1 was lower than cluster2. Among various clusters, the CIBERSORT algorithm analyzed 22 various types of immune cells. The outcomes showed that many cells accounted for a large section of immune cell infiltration (Figure 2D), such as the plasma cells, CD8 T cells, B cells naïve, T cells CD4, T cells CD4 memory activated, memory resting, T cells regulatory, NK cells resting, T cell follicular helper, natural killer (NK) cells activated, MI, M2 macrophages, dendritic cells resting, macrophages M0, eosinophils, dendritic cells activated, mast cells resting, mast cells activated, and neutrophils. Besides, the

Table 1. The multivariate analysis of the 17 lncRNAs

ID	*HR*	*HR.95L*	*HR.95H*	*p value*
AC139149.1	2.61	1.3	5.24	0.01
AC147651.1	1.78	1.07	2.98	0.03
AC073111.1	1.46	1.04	2.05	0.03
RPARP-AS1	1.37	1.15	1.63	0
U91328.1	1.99	1.14	3.47	0.02
AC003101.2	2.27	1.15	4.46	0.02
AL161729.4	1.27	1.02	1.59	0.03
AC019205.1	7.23	1.12	46.47	0.04
AP001619.1	1.57	1.1	2.24	0.01
AC026367.1	2.98	1.07	8.25	0.04
AC245041.1	1.35	1.1	1.65	0
AL512306.3	3.62	1.41	9.31	0.01
AC156455.1	1.16	1.06	1.27	0
ZKSCAN2-DT	1.33	1.1	1.61	0
NIFK-AS1	1.63	1.12	2.38	0.01
ATP2B1-AS1	4.09	1.34	12.43	0.01
AL138921.1	3.22	1.01	10.22	0.05

results showed that compared with cluster2, the levels of NK cells, B cell memory, and monocytes in cluster1 were remarkably lower. In addition, compared with cluster2 with a poor prognosis, cluster1 with better survival showed more M1, M2 macrophages and T cell CD4 memory activation. We found that the expression of specific immune cell types might be significantly inhibited or enhanced by m6A-related patterns, which might affect the immunotherapy response.

lncRNAs signature construction

We first studied the whole TCGA group m6A-related lncRNAs prognosis using univariate and multivariate regression analysis. Seventeen independent prognostic lncRNAs related to m6A were screened. The HR, 95%CI and p values for the multivariate analysis of the 17 lncRNAs are detailed in Table 1. Next, we divided the 407 patient samples into test group (n=202) and training group (n=205). Univariate Cox regression analysis and LASSO-penalized Cox regression analysis and were conducted to set up 6-lncRNA (U91328.1, AC003101.2, AC245041.1, AC156455.1, NIFK-AS1, ATP2B1-AS1) signature model in the training set based on the 17 lncRNAs (Figure 3A,B). The risk formula calculated the risk point of each patient in the training group, test group, and complete group: risk point=U91328.1* 0.123 + AC003101.2*0.266 + AC245041.1 * 0.345 +AC156455.1* 0.133 + NIFK-AS1 * 0.199 + ATP2B1-AS1 * 0.219. With the median risk point as the critical value, the low-risk set or high-risk set were distinguished. Figures 3C,3D showed that with the growth of the risk point, the OS of high-risk patients in the training set was remarkably lower than that of low-risk patients (p<0.001) and testing set (p=0.008). We observed the same results across the entire TCGA cohort

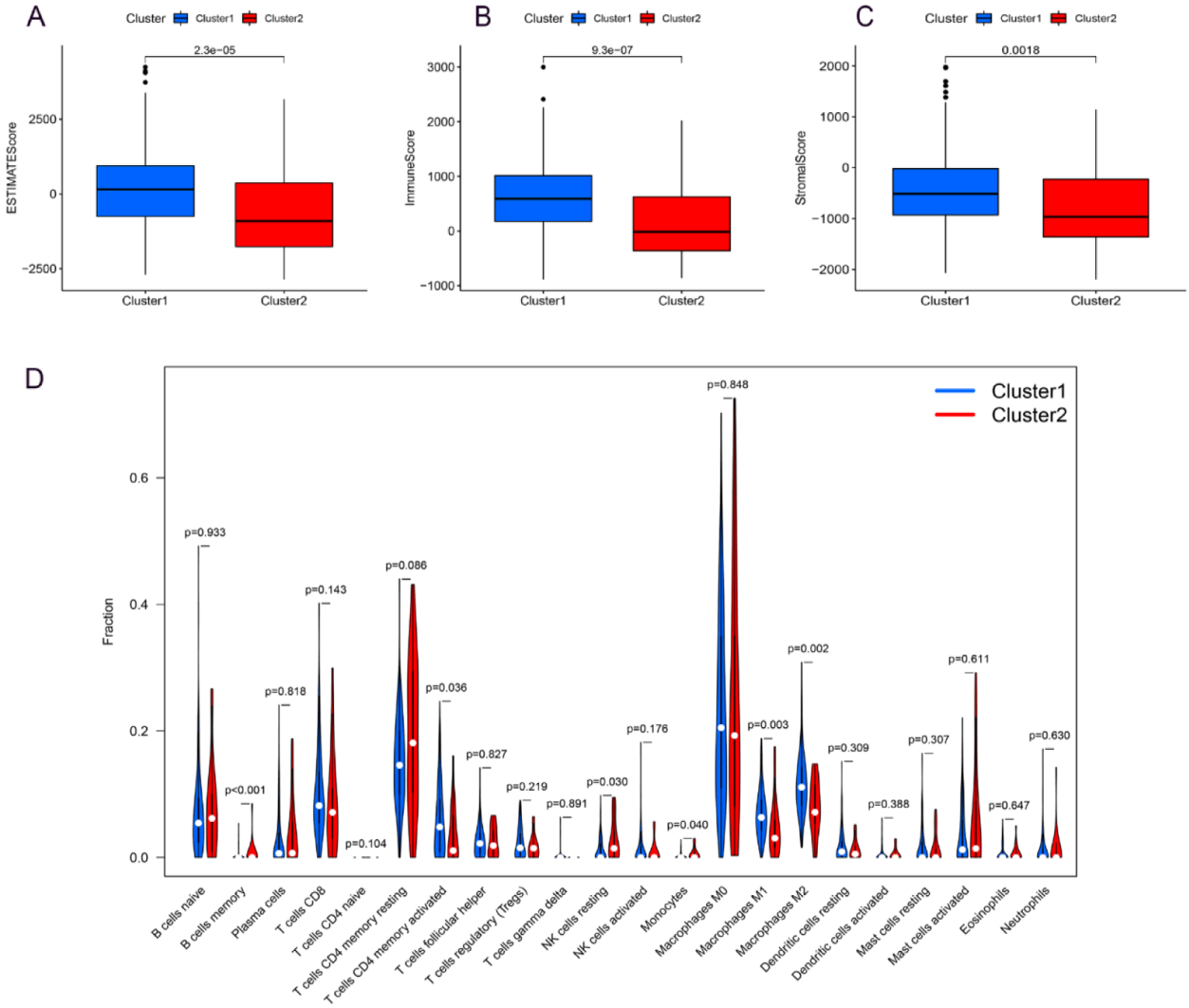

Figure 2. Immune infiltration between clusters. **A, B, C:** Various expression of ESTIMATE, immune and stromal score of three m6A clusters. **D:** Differences in the level of infiltration of 22 immune cells by two m6A clusters.

(Supplementary Figure 2A, p=0.008). What is more, in the testing data set, training data set, and complete data set, the area under the curve (AUC) of 5-year OS were 0.719, 0.738, and 0.724, respectively, indicating that there was a better accuracy in predicting the prognosis of GC (Figure 3E, 3F and Supplementary Figure 2B). Further on the study showed that the expression of these six lncRNAs was increased in all three groups. The patient risk score and the number of patient deaths were also positively correlated (Figure 4 and Supplementary Figure 3).

Independent prognostic role of the lncRNA signature

lncRNA expression and clinical elements were analyzed by univariate and multivariate Cox regression analysis to confirm the independence of the lncRNA characteristic (age, sex and clinical stage) in all three sets. As shown in Figure 5 and Supplementary Figure 4, it was discovered that for the COAD prognosis, the lncRNA characteristic could be considered as an independent element for prognosis. In order to in-depth forecast the prognostic model's ability, we analyzed the difference

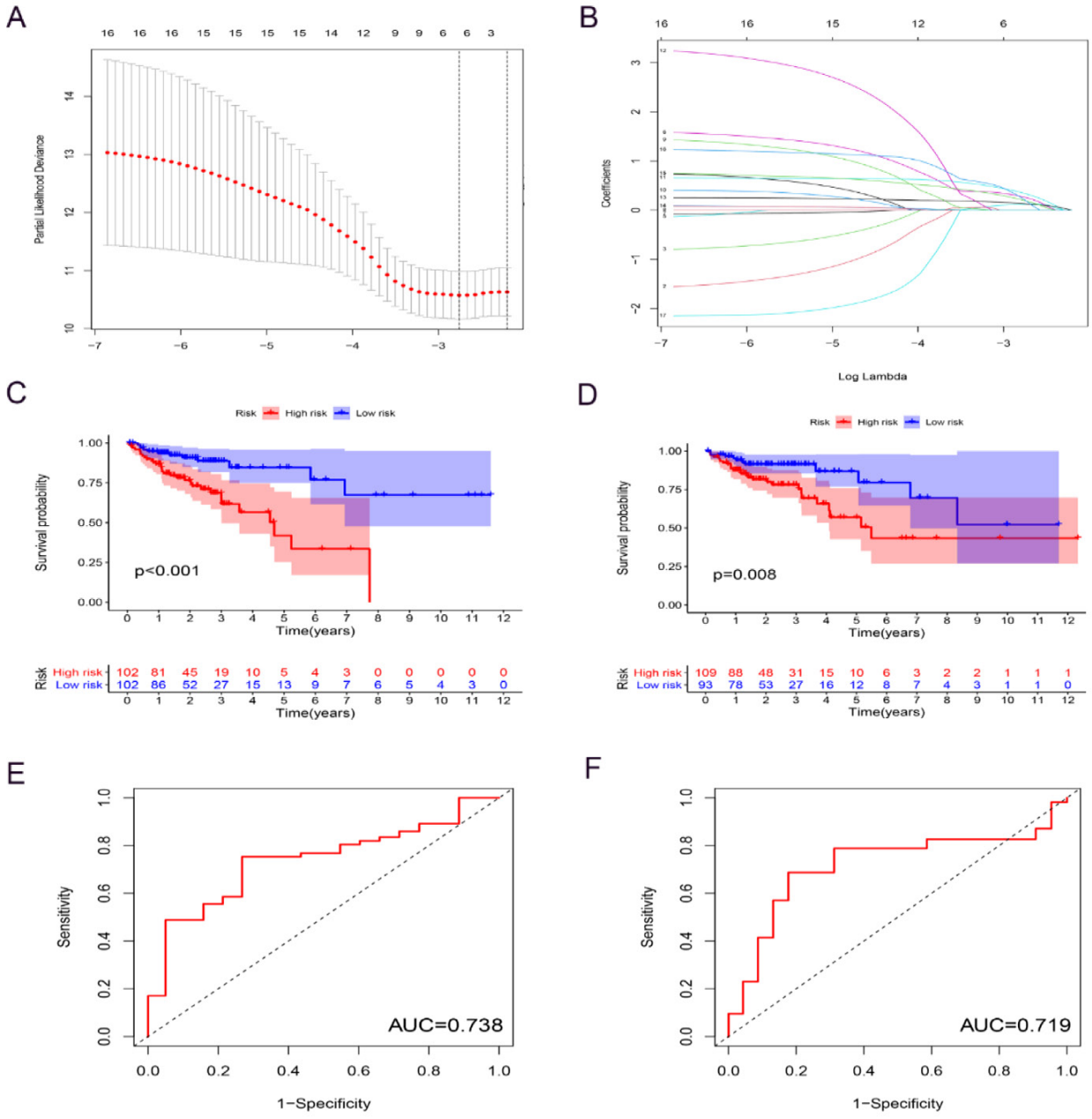

Figure 3. Risk model based on m6A-related lncRNAs. **A, B:** Lasso Cox regression analysis on 17 m6A-related lncRNAs. **C:** Patient's analysis of OS in high/low-risk groups in the training set. **D:** Patient's analysis of OS in high/low-risk groups in the testing set. **E:** ROC curve of the risk score in the training set. **F:** ROC curve of the risk score in the testing set.

of OS in the stratification of clinicopathological signature between the low-risk and the high-risk group. Classified by age, gender, stage and compared with the high-risk group, the low-risk group has better OS (Figure 6). The correlation between risk points and clinical signature and clustering has also been studied (Supplementary Figure 5). The results showed that there was a higher risk in the cluster, and a higher tumor stage was associated with a higher risk score. This confirmed our previous results that Cluster2 and advanced tumor stage had a worse prognosis. Therefore, these results suggested that the m6A-related lncRNA model was likely to be an excellent COAD prognosis.

Enrichment analysis

Through contrasting clusters with the threshold of logFC> 1 and adj. p < 0.05, we verified DEGs (Supplementary Table 2) to investigate the underlying biological distinction between the high and low-risk groups. The high-risk group had 548 up-regulated genes and 262 down-regulated genes compared with the low-risk group. In the GO analysis, biological processes showed the DEGs were abundant in ribonucleoprotein complex biogenesis and RNA splicing. The presence of abundant DEGs appeared in nuclear speck, and the cell-substrate junction was shown by cell component analysis. Analysis of molecular function suggested that

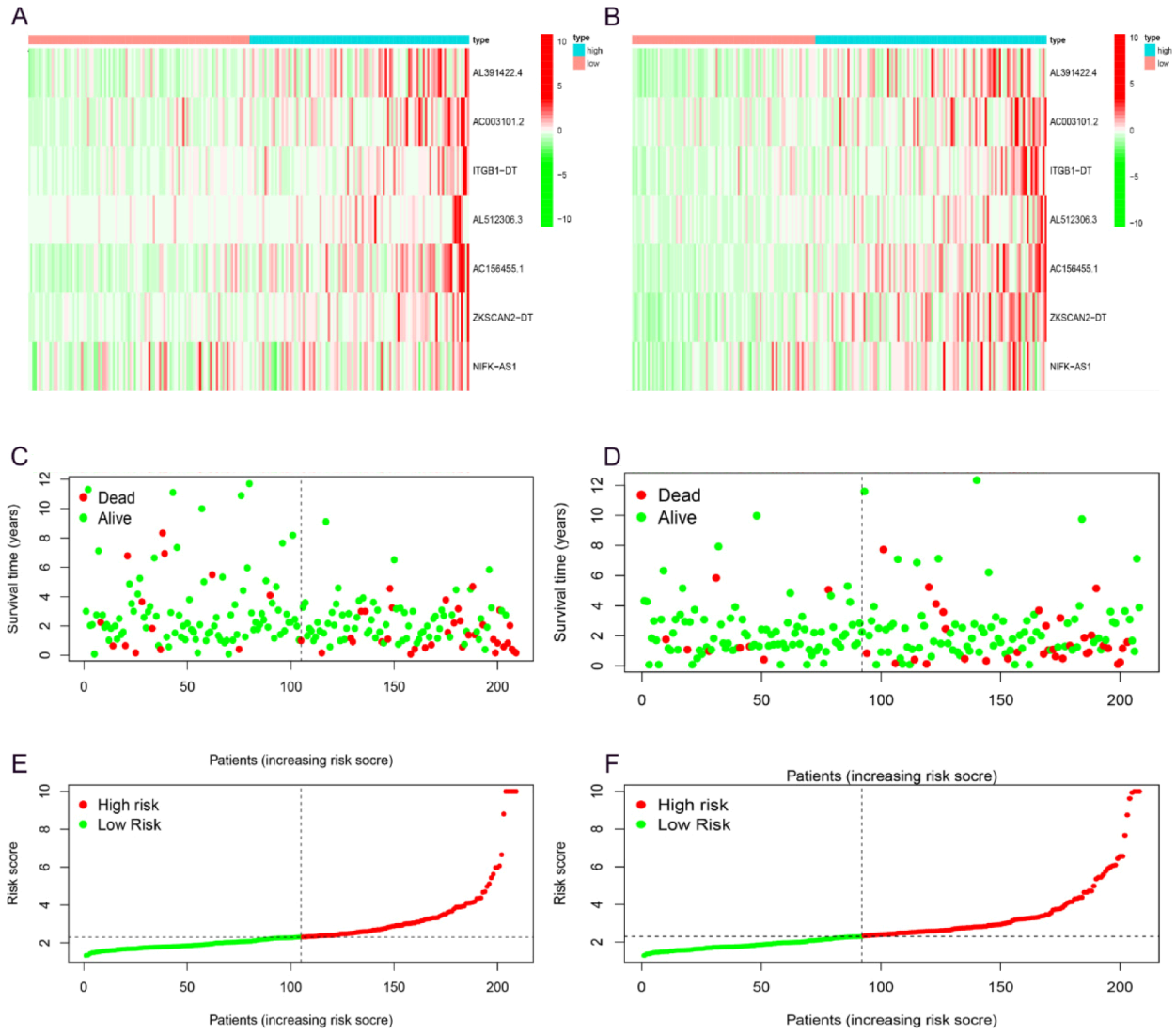

Figure 4. The prognostic value of 6 m6A -related lncRNAs risk patterns. **A:** Cluster analysis heat map of the expression criteria of 6 prognostic lncRNAs for each patient in the training set. **B:** Cluster analysis heatmap of the six prognostic lncRNAs expression criteria for each patient in the test set. **C:** Various modes of survival condition and survival time between the high- and low-risk groups in the training set. **D:** Various modes of survival condition and survival time between the high- and low-risk groups in the testing set. **E:** Allocation of m6A-related lncRNA model-based risk score in the training set. **F:** Allocation of m6A-related lncRNA model-based risk score in the testing set.

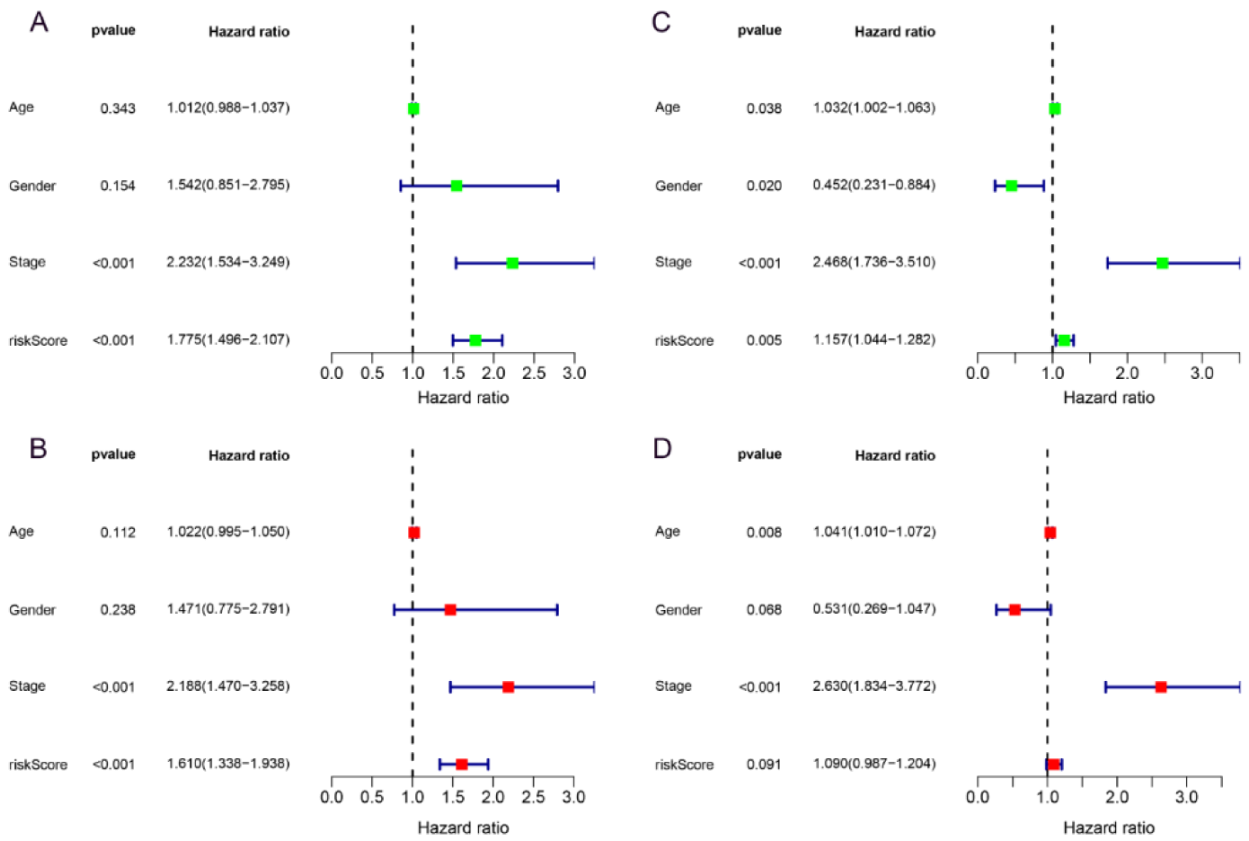

Figure 5. The independence of the m6A-related lncRNA signature in OS. **A:** Univariate Cox regression analysis in the training set. **B:** Multivariate Cox regression analysis in the training set. **C:** Univariate Cox regression analysis in the testing set. **D:** Multivariate Cox regression analysis in the testing set.

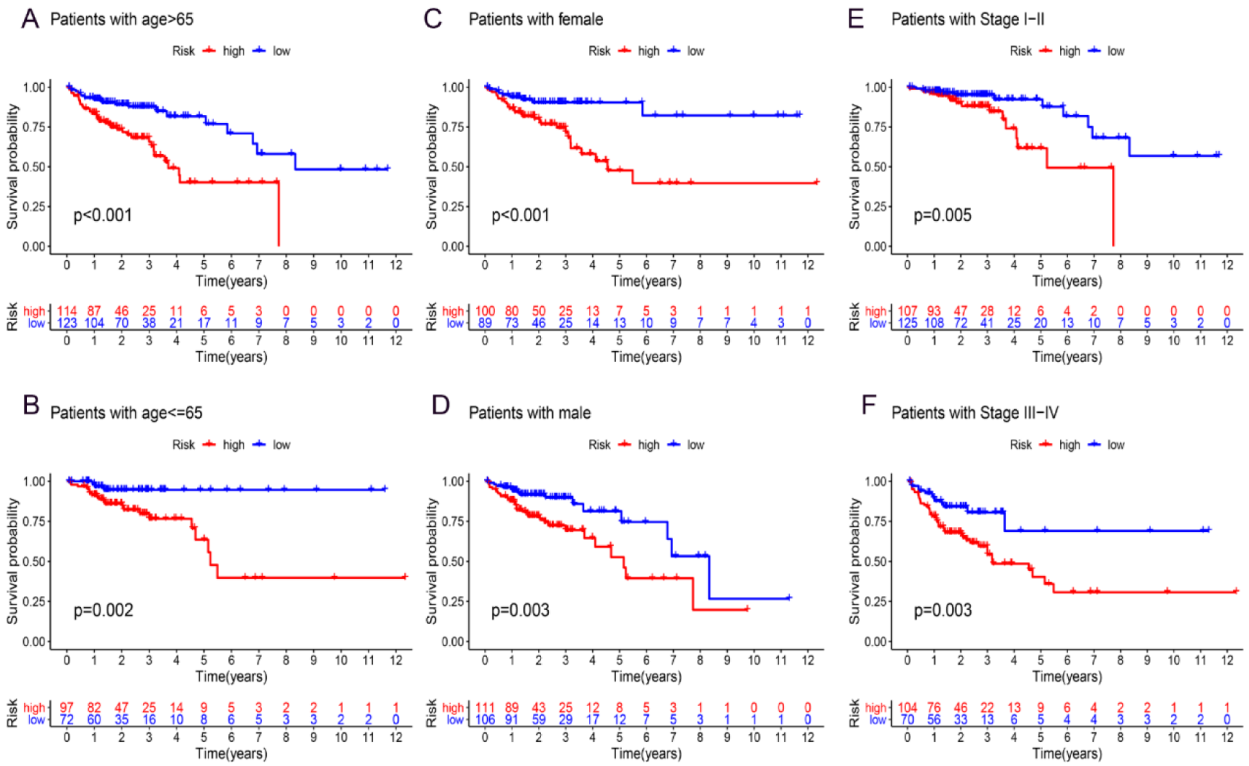

Figure 6. Kaplan-Meier survival curve of the high-risk group and low-risk group stratified by age and other clinical factors **(A, B)**, gender **(C, D)**, and stage **(E, F)** in the complete dataset.

DEGs were distributed in ATPase-coupled ion translation regulator activity and transmembrane transporter activity mainly. In addition, the analysis of KEGG revealed the DEGs were enriched in the spliceosome, mRNA surveillance pathway and oxidative phosphorylation and sulfur metabolism (Supplementary Figure 6A, 6B). There was a relationship between these signalling pathways and the carcinogenic process of core organisms, providing more therapy reference to the impact of m6A lncRNAs [20-23].

Construction and evaluation of the prognostic nomogram

To forecast the incidence of OS in 1, 2 and 3 years, we constructed a nomogram containing risk levels and clinical risk features. Through contrasting clinical elements, the nomogram presented the main predictive power of the prognostic model's risk level (Figure 7A). The 1-year, 2-year, and 3-year OS observation rate and prediction rate showed ideal agreement, which was shown by correlation graphs (Figures 7B-D).

Discussion

With the development of cancer research, it was gradually found that the traditional TNM staging system cannot fully explain the prognosis of all patients, and we need to develop a new prognostic marker. The conclusion that m6A-related lncRNAs were associated with a variety of tumors development has been reported by some authors [8,24,25]. Nevertheless, colon cancer research on m6A-related lncRNAs has been rarely studied systematically. This study explored the function of m6A-related lncRNAs comprehensively to forecast the survival and immunotherapeutic response in patients with COAD.

The matrix expressions of 23 m6A genes and 13150 lncRNAs in colon cancer were extracted from the TCGA database. Three clusters were determined based on the TCGA data set and the optimal k-means clustering method, and remarkable differences between the two clusters were observed in OS. This implied that m6A-related lncRNAs expression had a close correlation with the COAD malignancy and prognosis. Furthermore, our study showed no corre-

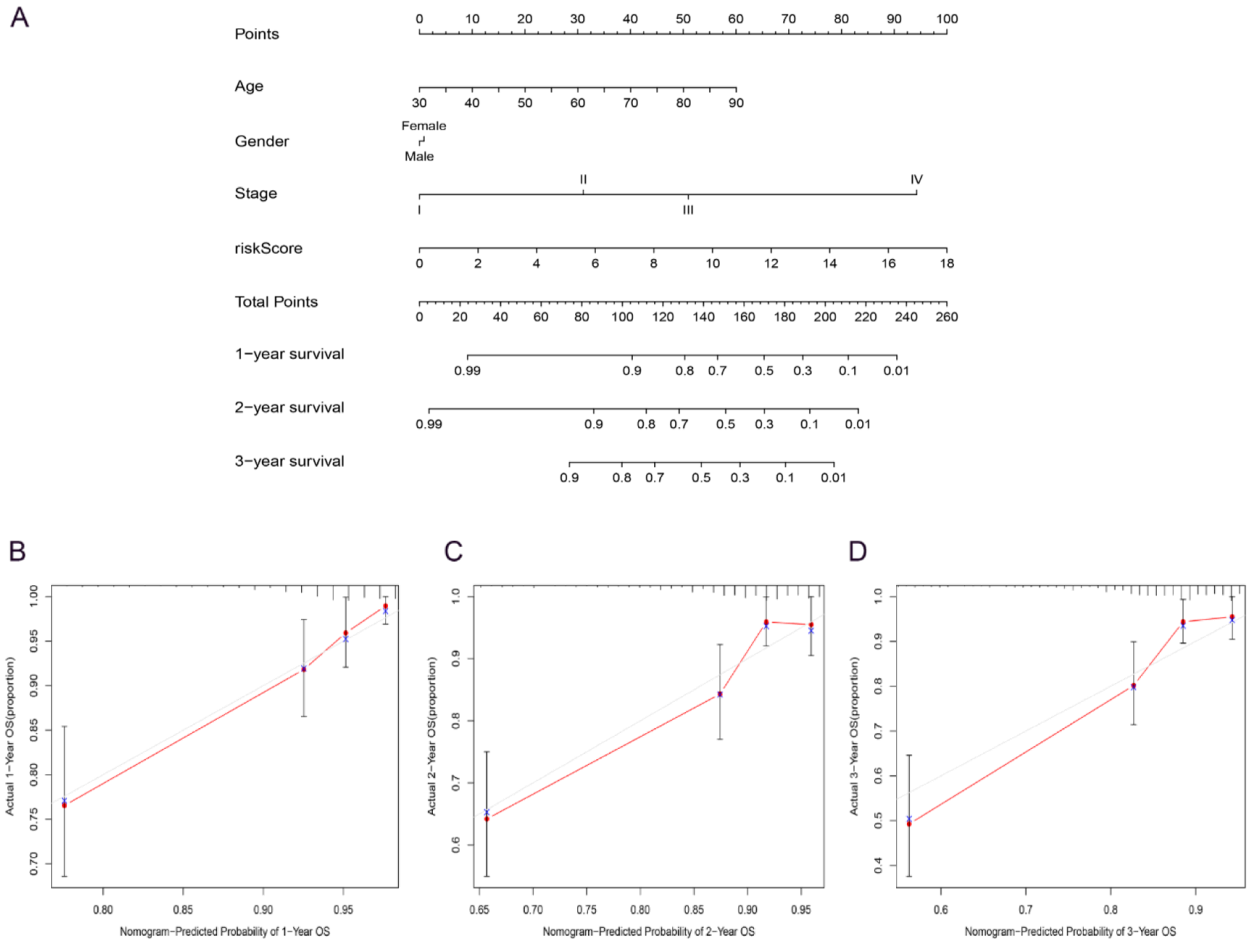

Figure 7. Construction and evaluation of a prognostic nomogram. **A:** The nomogram predicts the probability of the 1-, 2-, and 3-year OS. **B-D:** The calibration plot of the nomogram prediction of the probability of the 1-, 2-, and 3-year OS.

lation between clusters and clinical characteristics. People's understanding of the complexity of tumor microenvironment and the significance of tumor immunotherapy is gradually growing. Targeted specific immune checkpoints have generated great excitement due to their long-term efficacy [26]. We found no difference in PD-L1 expression between colon cancer and normal tissue, but group1 was significantly different from group2 with higher expression in group1, suggesting that patients in group1 were more likely to favor from immunotherapy. Further studies showed that most of the m6A-related lncRNAs had a correlation to PD-L1. Tumor cells and non-malignant cell tumors were involved in the tumor microenvironment (TME), such as tumor blood vessels, immune cells, fibroblasts, lymphatic vessels, vascular endothelial cells, and adipocytes. In tumor development's various processes, tumor immune cells exerted various functions, thus forming a dynamic immune system [27]. In our study, the ESTIMATE was remarkably different from the immune and stromal points between the m6A groups, with the highest point of cluster1. Compared with matrix, immune and ESTIMATE scores, tumor purity distributed differently, and tumor purity was usually opposite to the ESTIMATE score, so we inferred that the tumor purity score of cluster1 was lower than cluster2. This explains why cluster1 had a better prognosis. What is more, it was discovered that, compared with cluster2, cluster1 had a lower degree of NK cells, B cell memory, and monocytes. Furthermore, it was shown that cluster1 had more M1, M2 macrophages and T cells activated than those of cluster2. These results will help understand the TME cell infiltration features between clusters and through ensuring the action to immunotherapy, this will facilitate the individualization of new therapy.

Next, in COAD, the function of m6A-related lncRNAs prognostic was comprehensively studied. A 6 m6A-related lncRNA signature was successfully built with Cox univariate and multivariate regression analysis and LASSO-penalized regression analysis (U91328.1, AC003101.2, AC245041.1, AC156455.1, NIFK-AS1, ATP2B1-AS1). Few studies on these six lncRNAs have been published. The conclusion that this signature had a good prognostic value and could effectively classify the patient's OS was indicated by the results of the Kaplan-Meier analysis. In terms of forecasting COAD's 5-year OS, according to the results of further ROC analysis, lncRNA features had high accuracy. These outcomes showed that there was an excellent prognosis in the lncRNA signature. It might become an outstanding biological indicator for the COAD. The expression of these six lncRNAs was increased in all three groups. There was a positive correlation between the patient risk points and the number of patient deaths. This study applied univariate, multivariate and stratified analyses to find that the prognostic models were independent indicators for clinical features. Besides, the correlation between clinical elements and lncRNA signature was also assessed, showing that cluster2 had a higher risk score, and a higher tumor stage was associated with a higher risk score. This confirmed our previous results that Cluster2 and advanced tumor stage had a worse prognosis. Therefore, the above results suggested that the m6a-related lncRNA model had an excellent prognosis for COAD.

To investigate the underlying biological diversity among the high and low risk groups, analyses of GO and KEGG were conducted. The analysis of GO suggested the DEGs were abundant in ribonucleoprotein complex biogenesis and RNA splicing, ATPase-coupled ion transmembrane transporter activity, nuclear speck and cell-substrate junction, and translation regulator activity. The analysis of KEGG suggested the DEGs were enriched in the spliceosome, mRNA surveillance pathway and oxidative phosphorylation and sulfur metabolism. There was a relationship between the core biological carcinogenic process and these signalling pathways [21,22,28,29]. The above outcomes gave a clear orientation in COAD for elucidating the lncRNA signature's potential molecular mechanism. In addition, after a comprehensive analysis of OS factors, a nomogram was set up based on lncRNA signature, gender, age, and stage. The optimal performance of 1-year, 2-year, and 3-year OS was shown by the calibration chart, and this is possible to help propose the subsequent individual therapies.

In short, based on 6m6A-related lncRNAs, we established a prognostic model, and it had good clinical significance in its application. Some insufficiencies and limitations were also found in this study. To start with, this prognostic model lacked a large cohort or patient cohort and was built according to the TCGA database. Besides, more practical experiments are required to check the model accuracy to discuss lncRNA and its interaction with m6A-related lncRNAs.

Conclusions

In conclusion, most of the analyses studied the m6A-related lncRNAs expression and prognostic value. A high prognostic value 6-lncRNA signature was set up, and it could be regarded as an independent COAD prognostic indicator. The study on the development of the M6A-related lncRNA risk model in the COAD is presented for the first time.

New m6A-related lncRNAs perspectives were offered by this study, and personalized treatment was shown as well.

Additional information

Supplementary Figures and Tables are available at: https://jbuon.com/archive/26-5-C26925-Supplementary-materials.pdf.

Funding acknowledgements

This work was supported by Research project of National Natural Science Foundation of China (No: 81970358); Natural Science Foundation of Liaoning Province (1561449995778).

Conflict of interests

The authors declare no conflict of interests.

References

1. Sung H, Ferlay J, Siegel RL et al. Global Cancer Statistics 2020: GLOBOCAN Estimates of Incidence and Mortality Worldwide for 36 Cancers in 185 Countries. CA Cancer J Clin 2021;71:209-49.
2. Symeonidis D, Lazaris A, Zizi ZA et al. Correlation between LGR5 stem cells and location of tumor as well as age, sex and metastasis in colon adenocarcinoma. JBUON 2020;25:1827-31.
3. Hutchins G, Southward K, Handley K et al. Value of mismatch repair, KRAS, and BRAF mutations in predicting recurrence and benefits from chemotherapy in colorectal cancer. J Clin Oncol 2011;29:1261-70.
4. Tat T, Jurj A, Selicean C, Pasca S, Ionescu D. Antiproliferative effects of propofol and lidocaine on the colon adenocarcinoma microenvironment. JBUON 2019;24:106-15.
5. Alarcon CR, Lee H, Goodarzi H, Halberg N, Tavazoie SF. N6-methyladenosine marks primary microRNAs for processing. Nature 2015;519:482-5.
6. Chen XY, Zhang J, Zhu JS. The role of m(6)A RNA methylation in human cancer. Mol Cancer 2019;18:103.
7. Lan Q, Liu PY, Haase J, Bell JL, Huttelmaier S, Liu T. The Critical Role of RNA m(6)A Methylation in Cancer. Cancer Res 2019;79:1285-92.
8. Wang H, Meng Q, Ma B. Characterization of the Prognostic m6A-Related lncRNA Signature in Gastric Cancer. Front Oncol 2021;11:630260.
9. Sun M, Kraus WL. From discovery to function: the expanding roles of long noncoding RNAs in physiology and disease. Endocr Rev 2015;36:25-64.
10. Sun M, Gadad SS, Kim DS, Kraus WL. Discovery, Annotation, and Functional Analysis of Long Noncoding RNAs Controlling Cell-Cycle Gene Expression and Proliferation in Breast Cancer Cells. Mol Cell 2015;59:698-711.
11. Poursheikhani A, Abbaszadegan MR, Nokhandani N, Kerachian MA. Integration analysis of long non-coding RNA (lncRNA) role in tumorigenesis of colon adenocarcinoma. BMC Med Genomics 2020;13:108.
12. He PC, He C. m(6) A RNA methylation: from mechanisms to therapeutic potential. EMBO J 2021;40:e105977.
13. Shi H, Wei J, He C. Where, When, and How: Context-Dependent Functions of RNA Methylation Writers, Readers, and Erasers. Mol Cell 2019;74:640-50.
14. Yang Y, Hsu PJ, Chen YS, Yang YG. Dynamic transcriptomic m(6)A decoration: writers, erasers, readers and functions in RNA metabolism. Cell Res 2018;28:616-24.
15. Wilkerson MD, Hayes DN. ConsensusClusterPlus: a class discovery tool with confidence assessments and item tracking. Bioinformatics 2010;26:1572-3.
16. Newman AM, Liu CL, Green MR et al. Robust enumeration of cell subsets from tissue expression profiles. Nat Meth 2015;12:453-7.
17. Ashburner M, Ball CA, Blake JA et al. Gene ontology: tool for the unification of biology. The Gene Ontology Consortium. Nat Genet 2000;25:25-9.
18. Kanehisa M, Goto S. KEGG: Kyoto Encyclopedia of Genes and Genomes. Nucleic Acids Res 2000;28:27-30.
19. Iasonos A, Schrag D, Raj GV, Panageas KS. How to build and interpret a nomogram for cancer prognosis. J Clin Oncol 2008;26:1364-70.
20. Lee SC, Abdel-Wahab O. Therapeutic targeting of splicing in cancer. Nat Med 2016;22:976-86.
21. Wolin SL, Maquat LE. Cellular RNA surveillance in health and disease. Science 2019;366:822-7.
22. Ashton TM, McKenna WG, Kunz-Schughart LA, Higgins GS. Oxidative Phosphorylation as an Emerging Target in Cancer Therapy. Clin Cancer Res 2018;24:2482-90.
23. Hayes JD, Dinkova-Kostova AT, Tew KD. Oxidative Stress in Cancer. Cancer Cell 2020;38:167-97.
24. Jin Y, Wang Z, He D et al. Analysis of m6A-Related Signatures in the Tumor Immune Microenvironment and Identification of Clinical Prognostic Regulators in Adrenocortical Carcinoma. Front Immunol 2021;12:637933.
25. Xu F, Huang X, Li Y, Chen Y, Lin L. m(6)A-related lncRNAs are potential biomarkers for predicting prognoses and immune responses in patients with LUAD. Mol Ther Nucleic Acids 2021;24:780-91.
26. Sun C, Mezzadra R, Schumacher TN. Regulation and Function of the PD-L1 Checkpoint. Immunity 2018;48:434-52.
27. Baghban R, Roshangar L, Jahanban-Esfahlan R et al. Tumor microenvironment complexity and therapeutic implications at a glance. Cell Commun Signal 2020;18:59.
28. Campos-Melo D, Droppelmann CA, Volkening K, Strong MJ. RNA-binding proteins as molecular links between cancer and neurodegeneration. Biogerontology 2014;15:587-610.
29. Paluch EK, Aspalter IM, Sixt M. Focal Adhesion-Independent Cell Migration. Annu Rev Cell Dev Biol 2016;32:469-90.